

ON THE STRUCTURE OF QUASI-UNIVERSAL JETS FOR GAMMA-RAY BURSTS

NICOLE M. LLOYD-RONNING¹, XINYU DAI², BING ZHANG²¹Los Alamos National Laboratory, MS B244, Los Alamos NM, 87544; lloyd@cita.utoronto.ca²Department of Astronomy & Astrophysics, Pennsylvania State University, University Park, PA 16803;

xdai@astro.psu.edu, bzhang@astro.psu.edu

Draft version December 3, 2018

ABSTRACT

The idea that GRBs originate from uniform jets has been used to explain numerous observations of breaks in the GRB afterglow lightcurves. We explore the possibility that GRBs instead originate from a structured jet that may be quasi-universal, where the variation in the observed properties of GRBs is due to the variation in the observer viewing angle. We test how various models reproduce the jet data of Bloom, Frail, & Kulkarni (2003), which show a negative correlation between the isotropic energy output and the inferred jet opening angle (in a uniform jet configuration). We find, consistent with previous studies, that a power-law structure for the jet energy as a function of angle gives a good description. However, a Gaussian jet structure can also reproduce the data well, particularly if the parameters of the Gaussian are allowed some scatter. We place limits on the scatter of the parameters in both the Gaussian and power-law models needed to reproduce the data, and discuss how future observations will better distinguish between these models for the GRB jet structure. In particular, the Gaussian model predicts a turnover at small opening angles and in some cases a sharp cutoff at large angles, the former of which may already have been observed. We also discuss the predictions each model makes for the observed luminosity function of GRBs and compare these predictions with the existing data.

1. INTRODUCTION

One of the outstanding problems in the field of GRBs is understanding the extent to which these events are beamed, as well as the structure or configuration of the jet that produces the burst and its afterglow. The simplest model is a uniform jet, in which it is assumed that all parameters (density n , Lorentz factor Γ , magnetic and electron equipartition factors ϵ_B and ϵ_e , etc.) are constant throughout the jet. This jet can be described by an opening angle θ_j (or alternatively a solid angle $2\pi(1 - \cos\theta_j) \sim \pi\theta_j^2$). Under this assumption of uniformity throughout the jet, Frail et al. (2001) inferred the jet angle to a sample of GRBs with observed afterglows, from a break observed in the afterglow light curve. In a uniform jet model, this break occurs about the time when the GRB ejecta has slowed down enough so that the relativistic beaming angle of the radiation, $\sim 1/\Gamma$, becomes greater than θ_j (e.g. see Rhoads, 1997, Frail et al., 2001). Using the inferred jet angle, the measured flux and redshift to each burst, Frail et al. (2001), and then Bloom, Frail, & Kulkarni (2003; hereafter BFK) with a larger sample, were able to determine the emitted energy E of each burst. Remarkably, they found that the GRBs in their sample exhibited very little dispersion in E (see Figure 1 of BFK); in other words, they found that the isotropic equivalent energy of the GRB, E_{iso} , and the jet opening angle, θ_j , adhere to the relationship $E_{iso}\theta_j^2 \sim \text{constant}$. This intriguing result lends some credence to the possibility that a uniform description of a GRB jet may be valid.

However, an alternative model was suggested by Rossi et al. (2002) and Zhang & Meszaros (2002; hereafter ZM). They suggested that in fact GRBs may have a structured jet configuration, in which parameters such as the emitted energy can vary as a function of angle from the jet axis. All GRBs may then have approximately the same (“quasi-universal”) jet profile but appear different because of different orientations of the GRB jet to the observer (or in other words, varying observer angle θ_v). In this model, a break in the afterglow light curve is still ob-

served at the time the Lorentz factor slows to a value $\Gamma \sim 1/\theta_v$ (see Rossi et al., 2002, and ZM for more discussion). There are several advantages of this model. It has the appeal that it allows for uniformity among the GRB population, and also makes definite predictions about the distribution of observed break times in the GRB afterglow light curve (Perna, et al. 2003), as well as the observed GRB luminosity function (ZM). The uniform jet model has to require different bursts having different opening angles, and it has no predictive power for the observed distribution of these opening angles or the GRB luminosity function. In addition, realistic simulations (e.g. W. Zhang, Woosley & MacFadyen, 2002) naturally predict jet structure from the collapsar scenario, so it is essential to investigate the possible jet structures in the quasi-universal picture. Motivated by the Frail et al. result ($E_{iso}\theta_j^2 = \text{constant}$), the most straightforward universal jet model would be a power-law with an index of $k = -2$, as Rossi et al. and ZM have discussed. However, ZM observed that in terms of interpreting the lightcurves and jet breaks, one does not need to abide by any power-law jet configuration. In particular, they suggested that a Gaussian structure (and more general configurations) may describe the GRB jet. It has also been shown that a simple power-law model violates some of the observational data. For example, Granot and Kumar (2003), found that this type of model cannot reproduce the observed afterglow light curve, while Kumar and Granot (2003) have found that a Gaussian structure for the universal jet model does a better job.

In this paper, we test how well the quasi-universal jet model can reproduce the existing data. In particular, we test power-law and Gaussian models for the emitted energy, $\epsilon(\theta)$, as a function of angle from the jet axis. Because it is unphysical to expect that all GRBs have exactly the same jet structure, we allow for realistic scatter in the parameters of the models and place limits on this necessary scatter. The paper is organized as follows: In §2, we describe the data and any possible selection effects that may play a role in the results. In §3, we show how pure power-law

and Gaussian models fit the data of BFK. In §4, we introduce scatter into the parameters of each model and show how much dispersion is needed in these parameters to accurately reproduce the data. We also discuss predictions the Gaussian model makes in the $E_{iso} - \theta_j$ plane, which may be tested with future observations (and may have already been observed). In §5, we discuss what each model predicts for the observed luminosity function and how this compares to existing data. A summary and conclusions are presented in §6.

2. DATA

Our data is taken from BFK, which provides an isotropic energy estimate for 27 bursts. Of these bursts, 16 have a clear break in the afterglow light curve from which a jet opening angle (in the uniform jet model) can be inferred. These data are shown in Figure 1 (square points). Of the 11 bursts eliminated from the original sample, 8 have upper (or lower) limits to θ_j , based on a steeper (shallower) light curve observed at later (earlier) times, but no break directly observed. The other three bursts were well described by a single power-law throughout the extent of the observations. As discussed in the introduction, they found in this sample a very small dispersion for the energy emitted from a uniform jet of opening angle θ_j . This translates to a negative correlation between the isotropic equivalent energy E_{iso} and the jet opening angle, such that $E_{iso}\theta_j^2 \sim \text{constant}$. We performed all of our analysis below on both the nominal 16 bursts as well as the sample where the 8 limit bursts are included (where we took the limit as the nominal value), which gives us some idea of how eliminating these bursts biases the sample and our results. We find in fact the results do not change qualitatively or quantitatively in either case, so we consider our sample with the limits removed reasonably complete. We present results for the sample of 16 bursts for which a definite jet opening angle has been estimated.

Of course, there could be additional underlying selection affects biasing the entire sample that must be considered. This is a concern, for example, if there is a selection against detecting high E_{iso} , high θ_j bursts or low E_{iso} , low θ_j bursts. Such selection effects could produce an *artificial* correlation in the $E_{iso} - \theta_j$ plane. This latter bias could be particularly worrisome. First, a low θ_j implies an early jet break time, and a steepening of the light curve that may lead to a missed afterglow detection. More importantly, however, is that a low E_{iso} may be missed due to the flux limit of the detector. For a burst at some redshift z , the limit on E_{iso} is given by $E_{iso,lim} = F_{lim}4\pi d^2(1+z)$, where F_{lim} is the limiting fluence (time integrated flux) of the detector and d is the metric distance as a function of redshift. For bursts at a redshift of 1, for example, we find that $E_{iso,lim} \sim 10^{50}(F_{lim}/3 \times 10^{-8} \text{ergcm}^{-2}) \text{erg}$. This is well below the values of E_{iso} in our sample. [We also point out that there is some evidence that bursts have higher E_{iso} at higher redshifts (Lloyd-Ronning, et al. 2002, Amati et al., 2002, Yonetoku et al. 2003, Graziani, et al. 2003), which helps reduce the severity of the flux selection.] In addition, the expression for computing θ_j (see equation 1 of Frail et al., 2001) is very weakly dependent (to the 1/8 power) on E_{iso} . This means that the functional form of the truncation in the $E_{iso} - \theta_j$ plane goes as $E_{iso} \propto \theta_j^{-8}$, which is far steeper than the correlation observed. As a result, we conclude that selection effects are probably not producing the correlation between E_{iso} and θ_j in the BFK data, and that this is a reflection of a real physical effect in GRBs. Under the assumption that this correlation is real, we explore configurations of the energy as a function of angle $\epsilon(\theta)$ in the quasi-universal

configuration.

3. QUASI-UNIVERSAL JET MODELS

In the universal jet model, the observer angle θ_v takes the place of the jet opening angle θ_j . Then - as described in ZM - $E_{iso}(\theta_j)$ in the uniform jet model translates to $\epsilon(\theta)$, the energy as a function of angle from the jet axis, in the quasi-universal picture. In principle, we can then fit $E_{iso}(\theta_j)$ with various models to constrain the possible quasi-universal jet structure $\epsilon(\theta)$. As discussed in the introduction and in ZM, two plausible models for the jet structure $\epsilon(\theta)$ are a power-law and a Gaussian. We describe each in turn below.

3.1. Power-law

One possible model for the structure of a universal jet is a power-law:

$$\epsilon(\theta) = \epsilon_o(\theta/\theta_*)^{-k}, \quad (1)$$

for $\theta > \theta_c$, where θ_c is some cutoff to prevent divergence (see also ZM). The solid line in Figure 1 shows the best power-law fit to $E_{iso}(\theta_j) \propto \epsilon(\theta)$. The best fit gives an index k of -1.9 ± 1.1 . We emphasize that the reduced χ^2 of this fit is unacceptably high (~ 8) because of the intrinsic scatter in the data (we will return to this point when we compare Gaussian models to the data). Nonetheless, a simple power-law structure describes the general trend of the data well. Of course this result is not surprising since the Frail et al. (2001) and BFK result shows that $E_{iso}\theta^2 \sim \text{constant}$ (or $E_{iso} \propto \theta^{-2}$). Although this model appears to describe the data, it is worth investigating what other types of jet structure may produce the BFK data. In particular, Granot & Kumar (2003) ran simulations which showed that a power-law jet structure cannot reproduce the afterglow light curves - there is an unobserved flattening both right before the jet break and also at late times (after the jet break). A Gaussian, model, on the other hand, does reproduce the features observed in the afterglow lightcurves (Kumar & Granot, 2003). We explore this model in the next section.

3.2. Gaussian

A Gaussian model,

$$\epsilon(\theta) = \epsilon_o e^{-\theta^2/2\theta_o^2} \quad (2)$$

is also a physically reasonable suggestion for the structure of a universal jet. In this model, the energy peaks at $\theta = 0$ (i.e. down the center of the jet axis) and θ_o can be considered a characteristic width of the jet. The dotted line in Figure 1 shows the best fit Gaussian jet structure, with a characteristic jet width θ_o of 13 degrees. By eye, one can see that this is an unacceptable description of the data and indeed this is confirmed formally (with reduced $\chi^2 \sim 20$). [We note that when a Gaussian + power-law model is tried, the Gaussian component is made negligible in the fit routine, consistent with the above results.]

However, we point out that it is unphysical to expect that a jet's energy structure (as a function of angle from the axis) will be exactly the same from GRB to GRB. A much more natural and physical model is to allow a *quasi-universal* configuration - i.e. to allow some scatter in the parameters of each of these models. It is possible, then, that more general configurations (other than a simple power-law) can better describe the data. We explore this possibility in the following section.

3.3. Varying the Model Parameters

We investigate how the Gaussian and power-law models improve in describing the data when we allow the parameters (such as the power-law index or mean of the Gaussian distribution) to vary. We put limits on how much the parameters in each model much vary to reproduce the scatter in the observed data. As we will show below and as is consistent with our results in the previous section, a power-law model does a good job of describing the data and requires only small intrinsic scatter in the model parameters. However, the Gaussian model can also reproduce the observed data well; furthermore, in most cases this model predicts a sharp cutoff in the $E_{\text{iso}} - \theta_j$ plane at large θ_j as well as a turnover at very low values of θ_j , the latter of which may already have been observed. We discuss this in more detail below.

3.3.1. Method

To test this scenario, we allow one parameter (or two when noted) of each model to vary according to either a log-normal or normal distribution. For example we can allow the normalization of the Gaussian model ϵ_o to vary as a log-normal distribution rather than be a single fixed value. For each value of θ ,¹ we draw the normalization ϵ_o (in this example) from a log-normal distribution with some mean and scatter, and keep the mean of the jet width θ_o fixed to some value. We then compute the energy using this normalization and θ_o according to equation 2. Because the normalization is drawn from a distribution with some scatter, this will produce some scatter in the energy as a function of angle. The point is to find out how *much* scatter is needed in each parameter of the models to reproduce the data. Besides requiring the data to qualitatively *look* similar, by reproducing the energy range and scatter of the BFK data, for the Gaussian jet model we would like the simulated data to be fit by a power-law with an index consistent with the fit to the BFK data (~ -2), with a $\chi^2 \sim 4 - 10$ (similar to that of the data). Finally, we run a Kolmogorov-Smirnov (KS) test to check whether the two distributions (data vs. simulations) can be considered statistically similar.

We comment that for all parameters but the index k in the power-law model, the log-normal distribution is the probably the most physically reasonable distribution for adding dispersion to the parameters of each model. It accurately reflects the dynamic range of variation seen in the data and avoids unphysical negative values for the energy that can arise when a simple normal distribution is used for the parameter variations. Also, if GRBs from progenitors over a wide mass range, e.g. $10 - 300 M_{\odot}$, a log-normal distribution is more natural to describe the dispersion in the physical parameters. If, however, they arise from progenitors of a very narrow mass range, a normal distribution for parameter variations may be appropriate. Although (except for the power-law index k) we consider the log-normal variations to be physically more reasonable, we present the results for both distributions below; our figures, however, show only the results of the log-normal variations (except, again, for the power-law index k).

3.3.2. Results

1. Power law:

First, we explore how much scatter is necessary in the power-law model to reproduce the scatter of the BFK data. We

consider the case where the power-law index k in equation 1 is not a constant but derived from a normal distribution $\propto \exp^{-(k - \langle k \rangle)^2 / 2\sigma_k^2}$. We choose a mean $\langle k \rangle$ of -2 and explore various σ_k values that can reproduce the data. For a $\theta_* = 1^\circ$ in equation 1, a scatter of $\sigma_k \sim 0.7$ adequately reproduces the BFK data. This is shown by the circles in Figure 2 (the BFK data are the square points). The bottom line is that the scatter in the power-law index need be on the order of ~ 0.7 to reproduce the scatter in the BFK data. We also vary the normalization ϵ_o as a log-normal $\propto \epsilon_o^{-1} \exp^{-(\lg(\epsilon_o) - \langle \lg(\epsilon_o) \rangle)^2 / 2\sigma_{\lg(\epsilon_o)}^2}$. We find that a mean of $\langle \lg(\epsilon_o / 10^{50} \text{erg}) \rangle = 4.8$ and a dispersion $\sigma_{\lg(\epsilon_o / 10^{50} \text{erg})} = 0.6$ adequately reproduces the data (in the sense of reproducing the scatter and preserving the $k = -2$ power-law behavior) as shown by the circles in Figure 3. When we vary ϵ_o according to a normal distribution $\propto \exp^{-(\epsilon_o - \langle \epsilon_o \rangle)^2 / 2\sigma_{\epsilon_o}^2}$, we find that $\langle \epsilon_o / 10^{50} \text{erg} \rangle = 1.6 \times 10^4$ and $\sigma_{\epsilon_o} = \langle \epsilon_o \rangle$ does an adequate job of reproducing the scatter. In all cases, we have taken θ_* in equation 1 equal to 1° .

2. Gaussian:

In this case, we tried varying each of the parameters, ϵ_o and θ_o of the Gaussian model in equation 2, according to a log-normal and a normal distribution. For example, as described below, we let the dispersion or characteristic width of the jet θ_o be derived from a log-normal function with a mean $\langle \lg(\theta_o) \rangle$ and standard deviation $\sigma_{\lg(\theta_o)}$, while ϵ_o is fixed to some constant value. In addition, we try a model in which the normalization ϵ_o is taken from a log-normal distribution and then θ_o varies in a correlated way according to the equation $\epsilon_o \theta_o^2 \sim \text{constant}$. This is motivated by the fact that the Frail et al. (2001) and BFK data imply that the total GRB energy is approximately constant (in a uniform jet configuration); in the quasi-universal Gaussian model, this total energy is given by $\sim \epsilon_o \theta_o^2$ (ZM). A summary of our results are as follows:

- Varying the characteristic jet width, θ_o : We try a model in which θ_o in equation 2 varies as a log-normal with mean $\langle \lg(\theta_o) \rangle$ and standard deviation $\sigma_{\lg(\theta_o)}$. In general, we find that $\langle \lg(\theta_o / 1^\circ) \rangle$ in the range $0.7 - 0.8$ and $\sigma_{\lg(\theta_o)}$ in the range $0.3 - 0.5$ does the best job reproducing the data. A higher mean tends to create an unobserved flattening at low values of θ_j , while a lower mean causes the simulated data to be too steep (with power law index much steeper than -2). Figure 4 shows the simulated data vs. actual data in the BFK range for $\langle \lg(\theta_o / 1^\circ) \rangle = 0.8$ and $\sigma_{\lg(\theta_o)} = 0.4$. The simulated data shown in Figure 4 are fit with a power-law of index -1.8 ± 0.2 in the range of the BFK data; this is consistent with the index we obtained when fitting a simple-power-law to the BFK data. The fit gives a reduced $\chi^2 = 4.0$, which - although formally unacceptable - is consistent with the value of χ^2 obtained when we fit a power-law directly to the BFK data. Hence, we consider this similar value of k and χ^2 to indicate that we are accurately reproducing the slope and scatter of the data. Finally, when we perform a KS test on the simulated and observed data, we find that the probability that these data are derived from the same distribution is 69%. A very low value of this probability $\ll 1\%$ would indicate with statistical robustness that these data are from different distributions. Hence, we consider this model to adequately reproduce the data.

¹Our θ values are taken from the BFK data directly. However, we find qualitatively and quantitatively similar results if we draw our θ values from, say, a uniform distribution in linear space.

Using a normal distribution to produce variation in θ_o , with average value $\langle \theta_o \rangle$ and a standard deviation σ_{θ_o} , we find that values $\langle \theta_o \rangle \approx 7-10^\circ$ and $\sigma_{\theta_o} \approx 2-4^\circ$ do the best job in reproducing the data. Our best fit was for $\langle \theta_o \rangle = 9^\circ$ and $\sigma_{\theta_o} = 4^\circ$. The simulated data in this case are fit with a power-law of index -2.0 ± 0.2 in the range of the BFK data; this is consistent with the index we obtained when fitting a simple-power-law to the BFK data. The fit gives a reduced $\chi^2 = 6.4$. A KS test gives a probability of 15 % that these data are derived from the same distribution. In general, this particular model is quite unstable (for small variations in θ_o , we can get huge variations in the energy) and reproduces the data only in special cases.

- Varying the normalization, ϵ_o : We vary the normalization ϵ_o as according to a log-normal distribution with mean $\langle \lg(\epsilon_o) \rangle$ and standard deviation $\sigma_{\lg(\epsilon_o)}$. For a $\theta_o = 10^\circ$, $\langle \lg(\epsilon_o/10^{50}\text{erg}) \rangle$ in the range 3.4–3.7 and a $\sigma_{\lg(\epsilon_o/10^{50}\text{erg})}$ in the range 0.5–0.7 describes the data well. Figure 5 shows the simulated data for $\langle \lg(\epsilon_o/10^{50}\text{erg}) \rangle = 3.6$ and $\sigma_{\lg(\epsilon_o/10^{50}\text{erg})} = 0.7$. The simulated data shown in Figure 5 are fit with a power-law of index -1.5 ± 0.3 and $\chi^2 = 5.6$ in the range of the BFK data. The formal power-law fit is marginally consistent with the fit to the BFK data, but a KS test performed on the simulated and observed data sets gives a probability of 99 % that the two data sets are derived from the same parent distribution.²

When we vary the normalization ϵ_o according to a normal distribution with mean $\langle \epsilon_o \rangle$ and standard deviation σ_{ϵ_o} , we find that for a $\theta_o = 10^\circ$, $\langle \epsilon_o/10^{50}\text{erg} \rangle = 1.3 \times 10^3$ and $\sigma_{\epsilon_o} = 1.7 \times 10^3$ describes the data well. Note that the values of the mean and dispersion cause some deviates to be negative. In this case, we take the absolute value of all deviates. The data here are fit with a power-law of index -2.0 ± 0.2 and $\chi^2 = 7.4$ in the range of the BFK data. A KS test performed on the simulated and observed data sets gives a probability of 49 % that the two data sets are derived from the same parent distribution.

- Varying θ_o and ϵ_o in a correlated way: Finally, we vary θ_o and ϵ_o such that the total energy $\epsilon_o \theta_o^2 = \text{constant}$, again motivated by the result of Frail et al. (2001) and BFK that the total GRB energy is approximately constant. To do this, we take ϵ_o from a log-normal distribution as described in the previous section and solve for θ_o from the above relationship. We find the observed data is reproduced when $\langle \lg(\epsilon_o/10^{50}\text{erg}) \rangle = 3.4$ and $\sigma_{\lg(\epsilon_o/10^{50}\text{erg})} = 0.6$. This results in a mean jet width of 20° . The simulated data shown in Figure 6 are fit with a power-law of index -1.8 ± 0.2 and $\chi^2 \sim 6.6$ in the range of the BFK data. A KS test performed on the simulated and observed data sets gives a probability of 63 % that the two distributions are the same.

For a normal variation in ϵ_o , we find the observed data is reproduced when $\langle \epsilon_o/10^{50}\text{erg} \rangle = 1.3 \times 10^3$ and $\sigma_{\epsilon_o/10^{50}\text{erg}} = 2.0 \times 10^3$. This gives a mean jet width of about 10° . These simulated data are fit with a power-law of index -1.7 ± 0.2 and $\chi^2 = 4.4$ in the range of the BFK data. A KS test performed on the simulated and observed

data sets gives a probability of 21 % that the two distributions are the same.

The bottom line is that the data can be adequately reproduced with a Gaussian model for the jet structure, given some variation in the models parameters (we note that in our simulations, we have assumed that the viewing angle is the agent that determines the jet break time). Each model above was able to reproduce the power-law behavior of the BFK data, the scatter (reflected by the value of χ^2 of the power-law fit), and a KS test probability that shows that the simulated data are not inconsistent with being derived from the same parent distribution as the observed data. It appears, however, that the log-normal variations in ϵ_o and the correlated $\epsilon_o - \theta_o$ variations do the best job in reproducing the data (see Figures 5 and 6). The model in which θ_o varies in general exhibits too much curvature and is less stable to the degree of variation. Although the correlated $\epsilon_o - \theta_o$ variations do a good job of reprocing the data, the additional constraint that $\epsilon_o \theta_o^2 = \text{constant}$ may be considered an unattractive feature of this model. However, we do point out that this constraint is motivated by the observations (Frail et al., 2001, BFK) and may in fact be a physical feature of GRBs.

An interesting aspect of the Gaussian model is that the $k = -2$ power-law behavior is not extended below values of $\theta_j \lesssim 2^\circ$ and in some cases above $\theta_j \gtrsim 30^\circ$. Figure 7 shows simulations for the correlated $\epsilon_o - \theta_o$ variations, extended above and below the range of the BFK data. A turnover is clearly seen at low values of θ_j . For the case of either ϵ_o or θ_o varying individually, or for the case of the correlated $\epsilon_o - \theta_o$ with a *low value for the average jet width* $\lesssim 5^\circ$, we also find a cutoff at high values of $\theta_j \gtrsim 30^\circ$. We note that Figure 7 uses the same parameters as in Figure 6, where the average jet width is 20° . This average jet width can vary and this will affect exactly where the low angle turnover and high angle cutoff appear. Nonetheless, if this model were correct, then we should not see many more bursts with $\theta_j \lesssim 1^\circ$, and possibly also $\theta_j \gtrsim 30^\circ$. These predictions may be tested with future observations of GRBs, and in fact the low θ_j prediction may have already been seen. Interestingly, BFK discuss several outliers in their sample that appear to be “fast-fading” (possibly because the jet break occurred at very early times, implying a very small value for the jet opening angle θ_j) and sub-luminous relative to the rest of the sample. This is consistent with the trend predicted by the Gaussian jet structure at small values of θ_j .

4. LUMINOSITY FUNCTIONS

4.1. Predictions

One of the advantages to the quasi-universal jet configuration, is that it makes definite predictions for the observed luminosity function (LF) of GRBs. For example, as discussed in ZM, the isotropic luminosity function $N(\epsilon)$ at a given redshift can be determined from the burst angular distribution $N(\theta)d\theta \propto \sin\theta d\theta \propto \theta d\theta$. In the power-law model, $\theta \propto \epsilon^{-1/k}$, so that $N(\epsilon) \propto \theta d\theta/d\epsilon \propto \epsilon^{-(1-2/k)}$. For a Gaussian model, $N(\epsilon) \propto \epsilon^{-1}$. These predictions are derived in the case of no variations in the model parameters. We extend this analysis by simulating luminosity functions, allowing parameters to vary in our power-law and Gaussian models. Using the best fit parameters and variation schemes from the previous analysis, we simulate 500,000

²Again, we note that the KS diagnostic is intended to check whether two distributions can be considered statistically *different*. A value $\ll 1\%$ would indicate such a result. A higher value (like 99 %) does not necessarily indicate the model is any better than a lower value (like 50 %). All of our KS probabilities show that it is *not* the case that the simulated and observed data are derived from different distributions.

GRBs for each jet structure with the distribution of observing angle following $N(\theta_v)d\theta_v \propto \sin\theta_v d\theta_v$, and where the range of the observing angle is from 0° to 90° . Again, these simulations hold for luminosity functions at a given redshift.

4.2. Power-law Jet Structure

We first test our methods by simulating the GRB LF in the case where $\epsilon(\theta)$ is a simple power-law (with no parameter variations, and our best fit index of $k = -1.9$). As expected we obtain a slope of the LF of index ≈ -2 (solid line in Figure 8), consistent with the analytical expression of ZM and given above in §4.1. The minimum luminosity of $\sim 10^{51}$ erg is due to the upper boundary of the observer angle $\theta_v = 90^\circ$. We then simulate the cases where the power-law index k varies according to a normal distribution, and ϵ_o varies according to both normal and log-normal distributions. The results are shown as dotted, dashed, and dash-dotted lines in Figure 8, respectively. The luminosity functions obtained when we allow parameters to vary are similar to the simple power-law jet at the high luminosity end, being well described by a power-law of index -2 for more than three order of magnitudes. At the low luminosity end, however, the LFs tend to flatten. This flattening is a result of the low-luminosity cutoff present in the simple power-law case. For example, above the cutoff, when we allow parameters to vary there is a compensation between lower and higher luminosities that preserves the overall slope of the luminosity function. However, variations in the parameters near the cutoff cause some GRB luminosities to be pushed below the minimum luminosity, without compensation from GRBs of lower luminosity.

4.3. Gaussian Jet Structure

Again, we first simulate the luminosity function of a Gaussian jet, with fixed normalization, ϵ_o , and characteristic jet width, θ_o . The result is a powerlaw of slope -1 , shown by the solid line in Figure 9, and consistent with the analytical expression in §4.1. Note that this luminosity function has a maximum luminosity corresponding to an observer angle of 0° . We then vary the characteristic angle, θ_o , of the Gaussian jet according to a log-normal distribution. The simulated luminosity function is very similar to the luminosity function obtained from constant Gaussian jet model; it has a power-law index of -1 and an upper bound, shown as dotted line in Figure 9. Next, we consider the case where ϵ_o varies as log-normal. The result is shown by the dashed line in Figure 9. The luminosity function resembles the case of constant ϵ_o and θ_o on the low luminosity end, but steepens at high luminosities. This steepening is due to the same type of effect that caused the flattening at the low luminosity end in the power-law jet case (see §4.2 above) - variations in the parameters near the maximum luminosity cause some GRB luminosities to be pushed above the maximum, without compensation from GRBs of higher luminosity. We also simulate the luminosity function in the case where both ϵ_o and θ_o vary, but preserve the relation $\epsilon_o\theta_o^2 = \text{constant}$ (see §3). The luminosity function is shown as dash-dotted line in Figure 9. The LF in this case has a slightly flatter power-law index at low luminosities, with a clear break at $L \sim 10^{52}$ erg and a sharp steepening after that. This break occurs because an anti-correlated $\epsilon_o - \theta_o$ distribution causes an enhanced pile-up near $(\langle \lg(\epsilon_o) \rangle, \langle \lg(\theta_o) \rangle)$ in the $\epsilon - \theta$ plane, leading to a flattening of the LF at the corresponding luminosity. Finally, we simulate LFs from Gaussian jets where the parameters vary according to a normal distribution; the LFs are shown in Figure 10. The

qualitative behavior is similar to the log-normal variation case, although these LFs are steeper at the high luminosity end over a smaller dynamic range.

The luminosity functions in both the power-law and Gaussian jet structures have a definite change of power-law index when variations in the model parameters are included. Power-law jets produce LFs with a slope of -2 , but with a dramatic flattening at luminosities below about 10^{51} erg. Gaussian jets produce LFs with a slope of ~ -1 , although varying ϵ_o , and θ_o and ϵ_o in an anti-correlated way, causes the LF to steepen at high luminosities. In particular, the anti-correlated $\epsilon_o - \theta_o$ case with log-normal parameter variations produces a clear break at $\lesssim 10^{52}$ erg, above which there is a steepening with an index of ~ -2 .

4.4. Comparing with observed data

We would like to compare the predictions for the GRB luminosity function from the quasi-universal jet model of GRBs, with the observed GRB luminosity function. Unfortunately, we are not yet at the point where we can directly measure the GRB LF with any statistical certainty. This is because there are still on a handful (~ 33) of GRBs with measured redshifts, and determination of the LF requires large numbers (at least 100) of luminosities from a uniform sample (and a sample with complete and detailed knowledge of the selection effects).

Usually, the GRB LF is estimated by utilizing a large sample of GRBs with a measured flux distribution $n(f)$, assuming an underlying density distribution, $\rho(z)$, cosmological model, and then computing the luminosity function $N(L)$ through the equation $n(f)df = N(L)\rho(z)/(1+z)(dV/dz)dLdz$. Note that this assumes independence of the variables L and z , or - in other words - that the luminosity function does not evolve with redshift. Several studies have taken this approach to estimate the GRB LF. For example, Stern et al. (2003) - assuming a steep decline in the GRB source population above a redshift of 1.5 - find $N(L) \propto L^{-1.4}$ up to $L \sim 3 \times 10^{51}$ erg and then sharply declines after that. Schmidt (2002) - using various models for the GRB rate density based on the estimates for the global star formation rate - find that the GRB luminosity function can be described by a broken power-law with an index ~ -1 on the low luminosity end ($< 3 \times 10^{51}$ erg) and sharply declines after that, consistent with the Stern et al. results. [All luminosities quoted are the isotropic equivalent luminosities.] Although these results are fairly uncertain because they rely on the assumption of the underlying GRB rate density, they appear to be marginally consistent with predictions from the Gaussian jet structure. The power-law universal jet may also be consistent with these results if the data is fit with a single power-law such that the steepening of the LF above some break causes an overall steepening of the LF index, closer to -2 . [We note that recently, some attempts have been made to constrain the GRB LF based on the small sample of bursts with direct spectroscopic redshifts. For example, van Putten & Regimbau (2003) find that a log-normal description of the LF does a suitable job of describing the existing data.]

Although spectroscopic redshifts have only been obtained to a number of GRBs too small to determine a luminosity function directly, in recent years there has been evidence of so-called "luminosity indicators" (Fenimore & Ramirez-Ruiz, 2000, Reichart et al., 2001, Norris et al. 2001) from which luminosities of GRBs can be obtained. For example, Fenimore & Ramirez-Ruiz (2000) found a correlation between GRB luminosity and

the light curve variability (an estimate of the “spikiness” of the light curve) based on a small sample of bursts with measured redshifts. From this, they were able to obtain luminosities and redshifts to 220 GRBs. Because they used BATSE gamma-ray data and chose a flux limit to their sample, the selection effects were very well defined and therefore a luminosity function can be estimated. Fenimore & Ramirez-Ruiz assumed independence between L and z in their sample and found a luminosity function with a power-law index of approximately -2 , consistent with the power-law quasi-universal jet configuration. A more detailed analysis of this sample, however, shows that L and z are in fact correlated (Lloyd-Ronning, Fryer, & Ramirez-Ruiz, 2002, Yonetoku et al. 2003, Graziani et al. 2003); this correlation has to be accounted for to correctly determine a LF from the data. Lloyd-Ronning et al. did this by defining a variable $L' = L/\lambda(z)$, where $\lambda(z)$ parameterizes the correlation between L and z . They found a single power-law fit gives $N(L') \propto L'^{-2.2}$, while a broken power-law fit gives $N(L') \propto L'^{-1.5}$ for $L' < L'_o$ and $N(L') \propto L'^{-3.3}$ for $L' > L'_o$, where $L'_o = 5 \times 10^{51}$ erg. Again, there is no underlying assumption about the density distribution of GRBs in this analysis and the correlation between L and z present in the data has been accounted for. [We mention that in the context of the quasi-universal jet model, luminosity evolution could imply the overall normalization ϵ_o evolves with redshift, or that the characteristic opening of the jet θ_o evolves.] The single power-law result appears to be more consistent with the power-law quasi-universal jet structure, while the broken power-law result is better described by the (at least qualitative) predictions of the Gaussian case. Finally, Norris (2002) found - using the luminosities and redshifts obtained from the luminosity-lag relation, another luminosity indicator (Norris et al, 2001) - that the GRB LF scales as L^{-1} for low luminosities and $L^{-1.8}$ for high luminosities. This is very similar to the results we obtain for the LF from a Gaussian jet when ϵ_o and θ_o vary in an anti-correlated way.

Although some of the above results suggest the plausibility of a Gaussian jet structure for GRBs, the predictions of the quasi-universal jet model GRB LFs are better tested when more GRBs with redshifts are obtained and a direct GRB LF can be measured. This is a primary goal of the Swift satellite, to be launched in June of 2004.

5. SUMMARY AND DISCUSSION

In this paper, we have tested two possible models for a quasi-universal jet structure to a GRB. In particular, we attempt to reproduce the data of BFK who showed an anti-correlation between the isotropic emitted energy E_{iso} and the jet opening angle, θ_j derived in a uniform jet model, such that $E_{iso} \propto \theta_j^{-2}$. In the quasi-universal jet model (Rossi et al., 2002, ZM), in which the jet opening angle and total emitted energy are approximately the same for all GRBs, but the energy varies as a function of angle from the jet axis *within* a GRB, this correlation is a reflection of the energy profile $\epsilon(\theta)$ as a function of angle from the jet axis. Motivated by ZM, who suggested that this profile may take on different functional forms, we have tested how Gaussian and power-law models for $\epsilon(\theta)$ reproduce the BFK data. In particular, we have allowed for realistic scatter in the parameters of each model (letting each parameter vary as a either a log-normal or normal distribution with some mean and standard deviation).

We find that both the power-law and Gaussian jet structures can reproduce the data quite well, with only minimal scatter

required in the model parameters - particularly when the parameters vary according to the more physically reasonable log-normal distribution. The strengths of the power-law model are its simplicity and ease in reproducing the observed data. However, as discussed in the introduction and throughout the text, there are several reasons to consider other jet configurations, and in particular the Gaussian model appears to adequately describe the observations. Furthermore, The Gaussian model predicts a sharp turnover in the $E_{iso} - \theta_j$ plane for low (and in some cases high) values of θ_j . This turnover at low jet angles has possibly been observed by BFK, who found a few “sub-luminous” bursts (relative to the rest of their sample), with steeply declining light curves which could indicate a very small opening angle θ_j . These “outliers” are consistent with the trend predicted by the Gaussian quasi-universal jet configuration at low θ_j . Furthermore, these outlier bursts challenge the BFK conclusion that the energy reservoir in GRBs is approximately constant, when taken in the context of the uniform jet model. However, the measured θ_j is - in the context of the quasi-universal jet paradigm - the *viewing* angle and not the characteristic width of the jet θ_o , which could be larger. This means that the total energy within the GRB could still be standard, if the results are considered in the quasi-universal jet picture with a *Gaussian* jet structure. We also find that the luminosity function predicted by the Gaussian model, including variations in the model parameters, appears to be consistent with past studies of the luminosity GRB LF, although these predictions are better tested when the GRB LF can be directly measured.

Perna et al. (2003) showed that a universal jet model with a power-law structure (of index of -2) predicts a distribution of break times in the afterglow light curve that is consistent with what is observed. It would be interesting to explore their analysis in the context of the Gaussian model, which is proving to be a viable model for the quasi-universal jet structure of GRBs. (Given our results above, we suspect that a Gaussian model may give qualitatively similar results as the power-law.) We note that Lamb et al. (2003) have recently pointed out that the quasi-universal jet model fails to reproduce the large dynamic range of the observed relationship between isotropic energy and spectral peak energy (see, e.g., Amati et al., 2002), which spans not only the “classic” GRB energies (i.e., those of BATSE, from ~ 50 keV to 1 MeV), but also includes so-called X-ray flashes, which have spectral peak energies down to a few keV. Their conclusions are in the framework of a power-law structure for the quasi-universal jet, and such an investigation in the framework of the Gaussian model is underway (Zhang et al., in prep). Furthermore, we comment that the realistic jet structure might not be strictly power-law, Gaussian, nor their simple superpositions; in fact, recent numerical simulations (Zhang, Woosley, & MacFadyen, 2003) indicate a double Gaussian structure for the jet may provide the best description (where one Gaussian is used for the core of the jet and one for the wings). The bottom line is now that we can reproduce the data with varying parameters in these simplified models, we can do it with more realistic models too. And such models may be able to explain all of the observed gamma-ray burst data in the context of a quasi-universal jet configuration.

We would like to thank Dale Frail for sending us a table of the BFK data. We would also like to thank the referee for insightful comments and suggestions that improved this work.

REFERENCES

- Amati, L. et al., 2002, *A&A*, 390, 81
Bloom, J. S., Frail, D., Kulkarni, S. 2003, *ApJ*, accepted (BFK)
Frail, D. et al. 2001, *ApJ*, 562, 55
Fenimore, E. E., & Ramirez-Ruiz, E. 2000; astro-ph/0004176
Granot, J. & Kumar, P. 2003, *ApJ*, 591, 1086
Graziani, C. et al., 2003, presentation at GRB2003
Kumar, P. & Granot, J. 2003, *ApJ*, 591, 1075
Lamb, D.Q., Donaghy, T.Q. & Graziani, C. 2003, presentation at GRB2003
Lloyd-Ronning, N.M., Fryer, C. L., & Ramirez-Ruiz, E. 2002, *ApJ*, 574, 554
Norris, J. P., Marani, G. F., & Bonnel, J. T. 2000, *ApJ*, 534, 248
Norris, J.P. 2002, *ApJ*, 579, 386
Perna, R., Sari, R. & Frail, D., 2003, *ApJ*, accepted.
Rhoads, J. 1997, *ApJ*, 487, L1
Rossi E., Lazzatti, D. & Rees, M.J., *MNRAS*, 332, 945
Schmidt, M. 2002 *ApJ*, 552, 36
Stern, B.E., Tikhomirova, Ya.; Svensson, R. 2002, *ApJ*, 573, 75
van Putten, M.P.H & Regimbau, T. 2003, *ApJL*, accepted
Yonetoku, D., et al. 2003, submitted to *ApJ*; astro-ph 0309217
Zhang, B. & Meszaros, P. 2002, *ApJ*, 571, 876 (ZM)
Zhang, W., Woosley, S.E., MacFadyen, A.I. 2003, *ApJ*, 586, 356

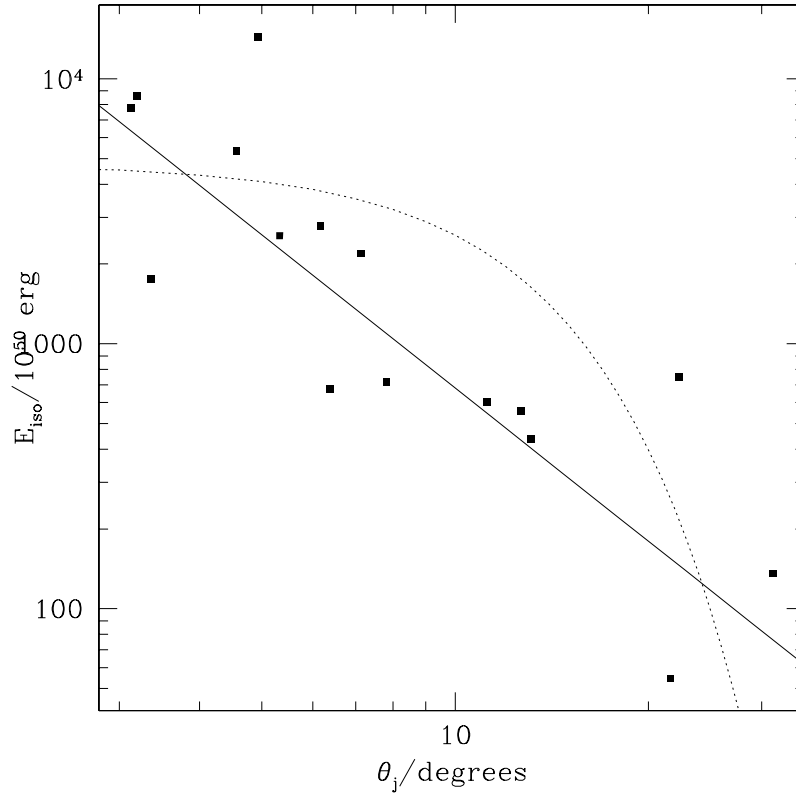


FIG. 1.— Isotropic emitted energy vs. jet opening angle. The square points are the data from BFK, the solid line shows a power-law fit to the data, while the dotted line shows a Gaussian fit.

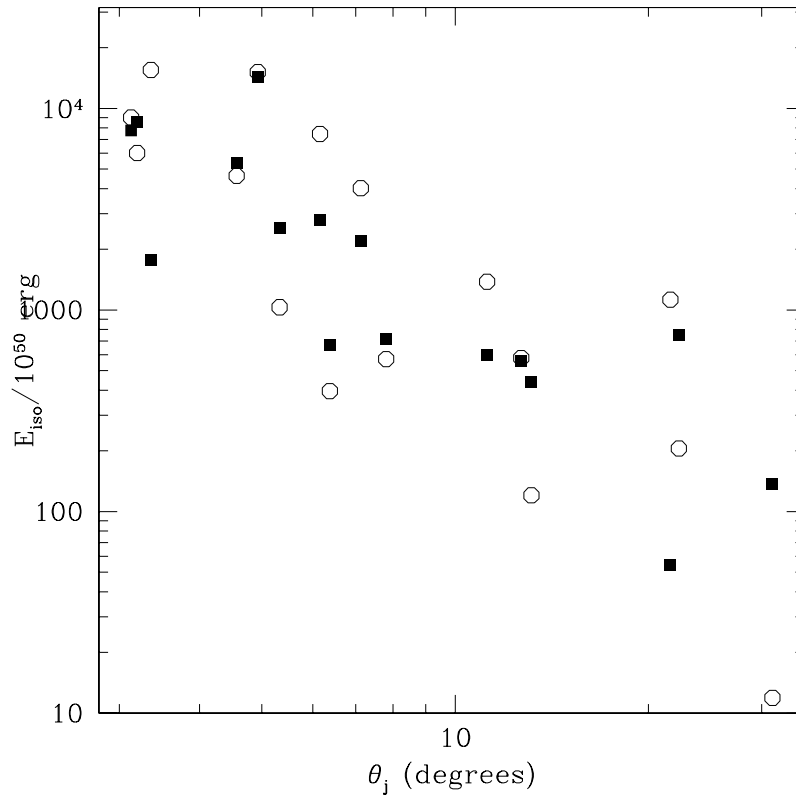


FIG. 2.— Isotropic emitted energy vs. jet opening angle. The square points are the BFK data, while the circles indicate data derived from a power-law jet structure, with an index k that varies according to a normal distribution with mean of -2 and standard deviation of 0.7 .

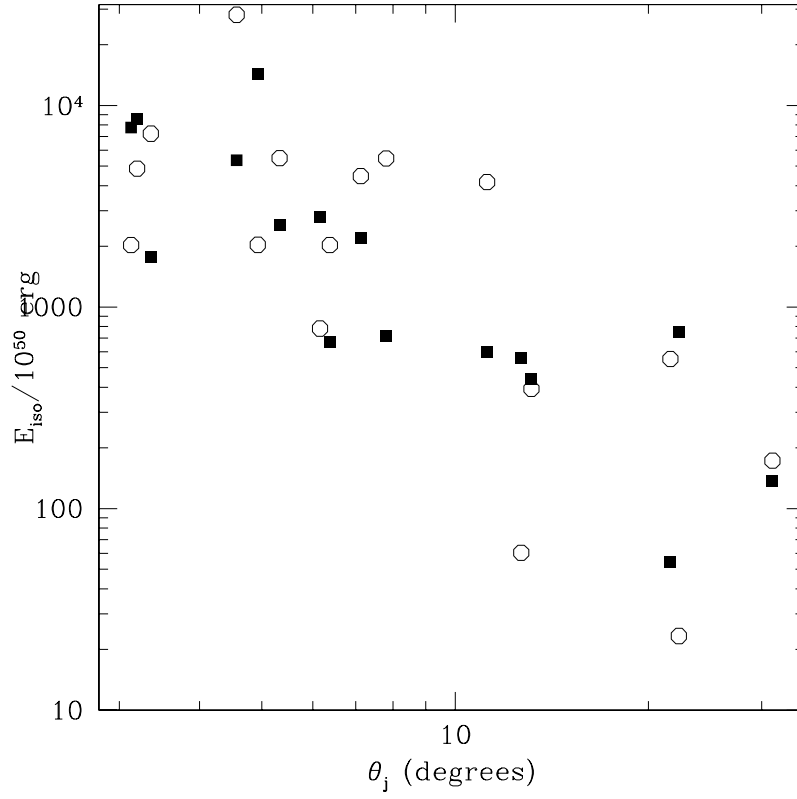


FIG. 3.— Same as Figure 2, but where the circles indicate data derived from a power-law jet structure, where the normalization varies as a log-normal distribution, with a mean $\langle \lg(\epsilon_o/10^{50} \text{ erg}) \rangle = 4.8$ and a standard deviation $\sigma_{\lg(\epsilon_o/10^{50} \text{ erg})} = 0.6$.

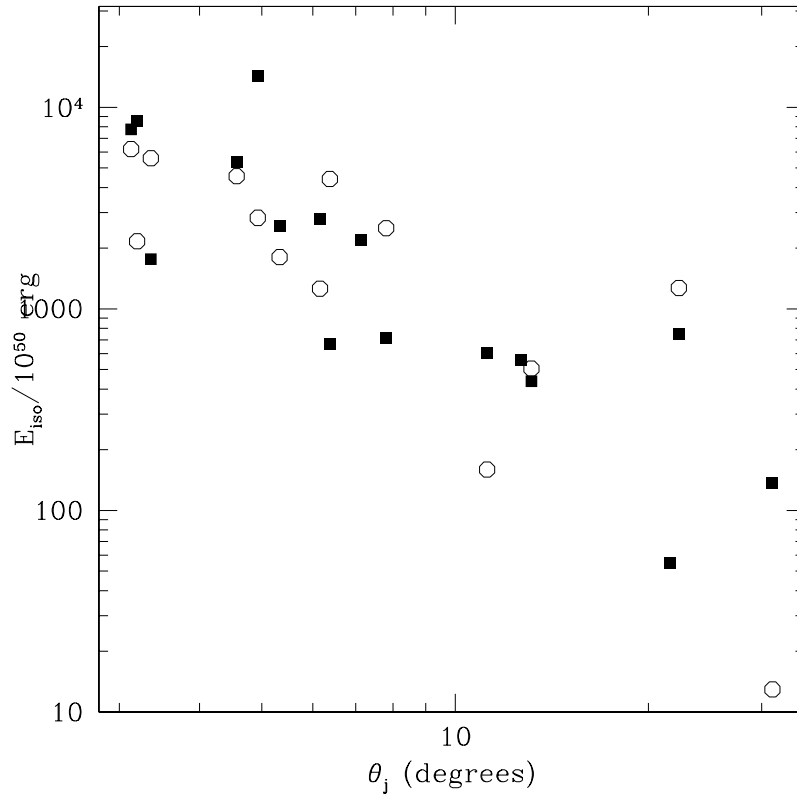


FIG. 4.— Same as Figure 2, but where the circles are data derived from a Gaussian jet structure, with a characteristic width θ_o that varies as a log-normal distribution with a mean $\langle \lg(\theta_o/1^\circ) \rangle = 0.8$ and a standard deviation $\sigma_{\lg(\theta_o/1^\circ)} = 0.4$.

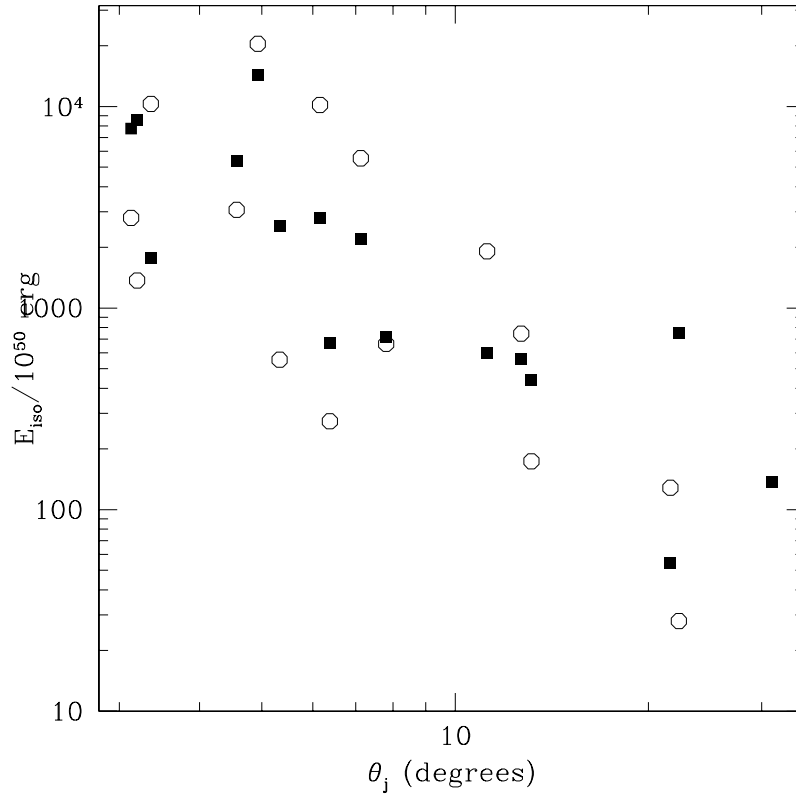


FIG. 5.— Same as Figure 2, but where the circles are data derived from a Gaussian jet structure, with a characteristic width $\theta_o = 10^\circ$ and a normalization ϵ_o that varies as a log-normal with a mean $\langle \lg(\epsilon_o/10^{50} \text{ erg}) \rangle = 3.6$ and a standard deviation $\sigma_{\lg(\epsilon_o/10^{50} \text{ erg})} = 0.7$.

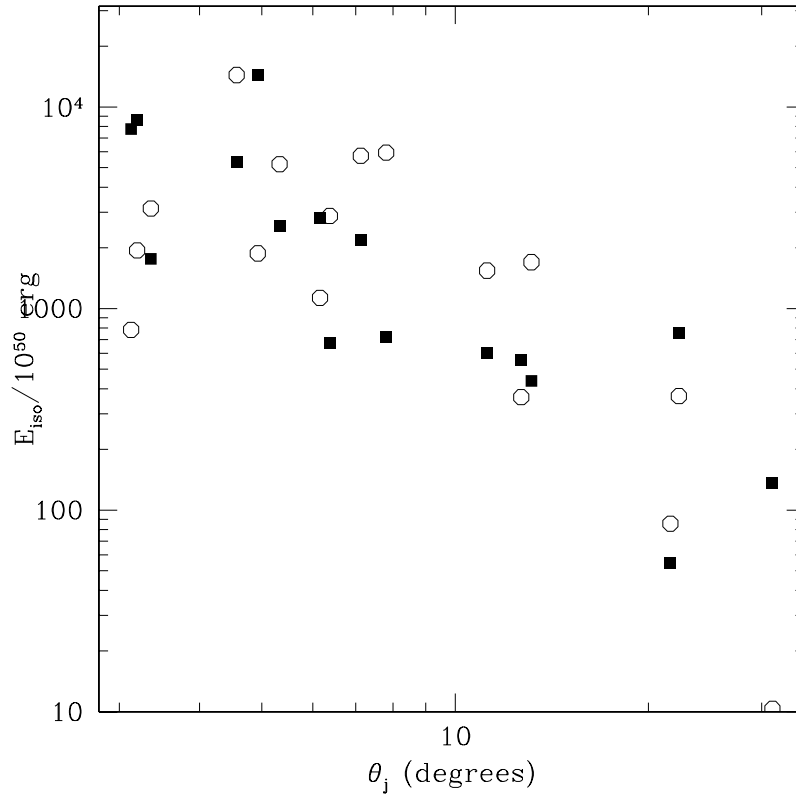


FIG. 6.— Same as Figure 2, but where the circles are data derived from a Gaussian jet structure, a normalization ϵ_o that varies as a log-normal with a mean $\langle \lg(\epsilon_o/10^{50} \text{ erg}) \rangle = 3.4$ and a standard deviation $\sigma_{\lg(\epsilon_o/10^{50} \text{ erg})} = 0.6$, and a characteristic jet width that follows the relation $\epsilon_o \theta_o^2 = \text{constant}$.

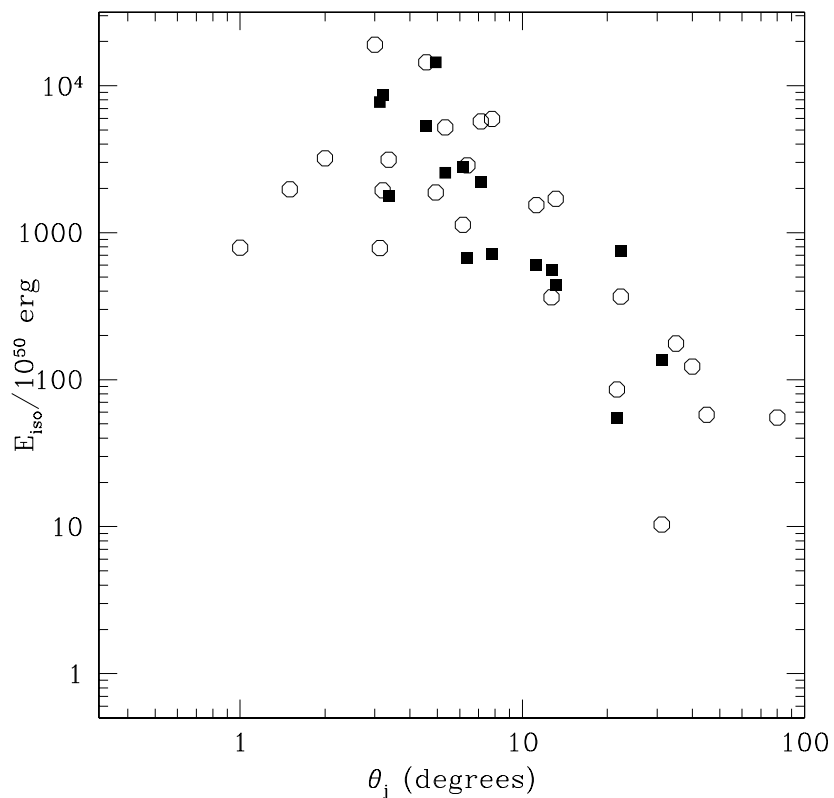


FIG. 7.— Same as Figure 6, but plotted over a larger range in both axes to show the turnover at low θ_j . For the case of $\langle \epsilon_0 \rangle$ or $\langle \theta_0 \rangle$ varying individually, there is also a sharp cutoff at high $\theta_j \gtrsim 30$ degrees.

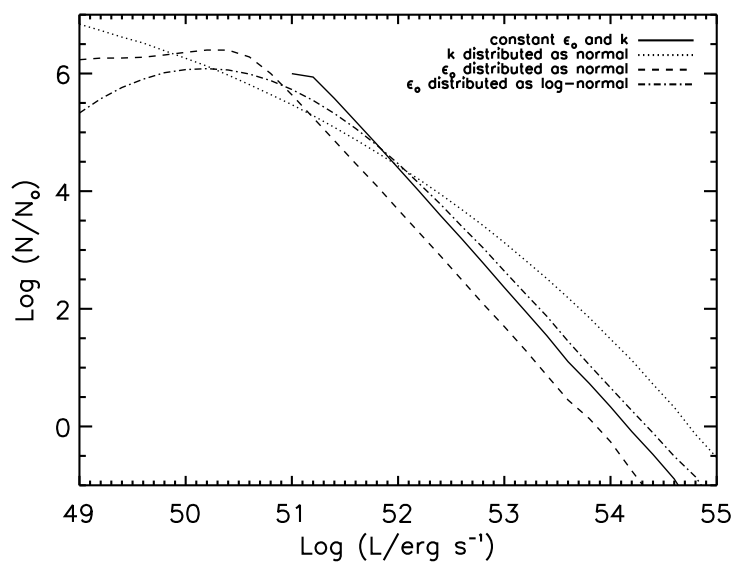


FIG. 8.— Monte-Carlo simulated (differential) luminosity functions for GRBs with power-law jets, where N_0 is an arbitrary normalization. The luminosity function is calculated assuming isotropic emission and a typical duration to all bursts. The solid, dotted, dashed, and dash-dotted lines represent power-law jets with no variations, with powerlaw index k varying as according to a normal distribution, with ϵ_0 varying as according to a normal distribution, and with ϵ_0 varying as a log-normal, respectively.

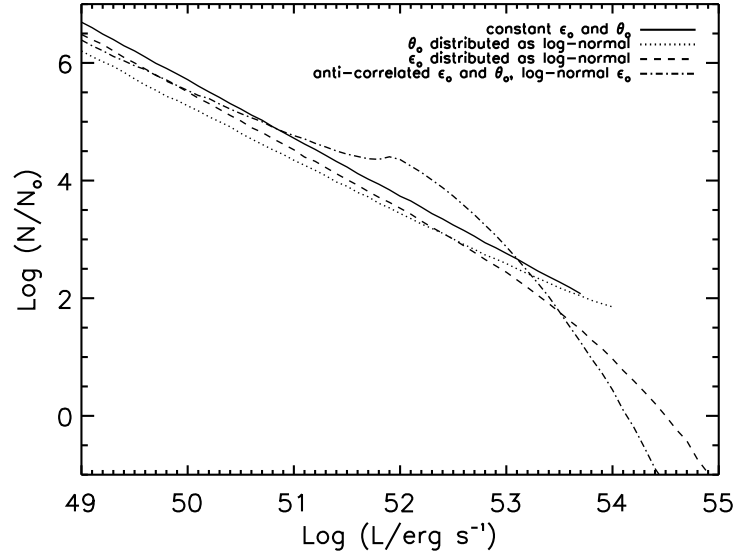


FIG. 9.— Same as Figure 8, but for Gaussian jets and log-normal parameter variations. The solid, dotted, dashed, and dash-dotted lines represent Gaussian jets with no variations, with θ_0 varying, with ϵ_0 varying, ϵ_0 and θ_0 varying in an anti-correlated way, respectively.

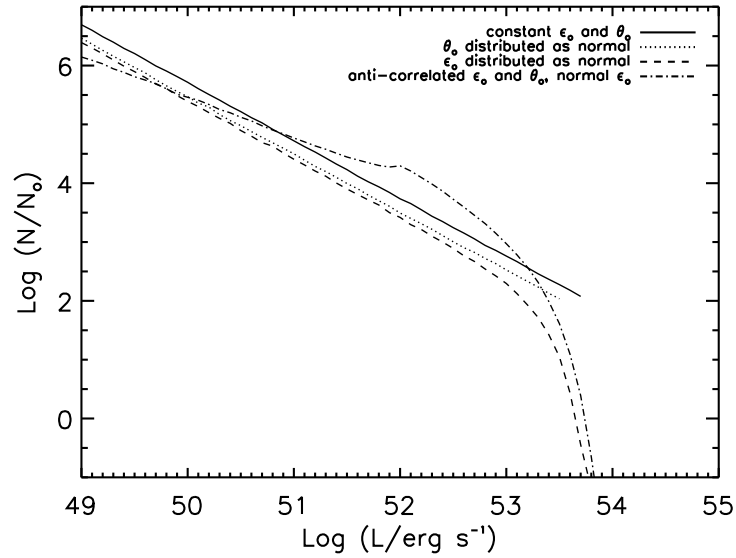


FIG. 10.— Same as Figure 9, but with the parameters varying according to a normal distribution.